JOURNAL OF SOLID STATE CHEMISTRY 74, 385–392 (1988)

Solid Electrolytes Based on Na_3PO_4:M^{4+} (M = Zr, Hf, Ti, Sn, Ce, Th)

J. T. S. IRVINE AND A. R. WEST

University of Aberdeen, Department of Chemistry, Meston Walk, Aberdeen AB9 2UE, United Kingdom

Received September 15, 1987; in revised form December 30, 1987

γ-Na_3PO_4 solid solutions have been prepared containing a range of tetravalent ions; the replacement mechanism is $4Na \rightleftharpoons M$. Approximate phase diagrams have been determined for each system, showing the extent and thermal stability of the γ solid solutions. For each system, lattice parameters were measured as a function of composition and conductivities were measured for several compositions over the temperature range 70–450°C. Solid solutions which were found to be the most extensive and which had the highest conductivities ($>10^{-2}$ ohm^{-1} cm^{-1} at 300°C) were for M = Zr, Hf; these systems also showed the smallest change of lattice parameter with composition.

Introduction

In searching for possible alternative Na^+ ion conductors to β-alumina, some attention has been given to Na_3PO_4 and its derivatives, mainly because the conductivity of Na_3PO_4 can be increased considerably by doping. Na_3PO_4 is a versatile structure and can be doped with divalent (Ca, Sr, Cd, Zn), trivalent (Al), tetravalent (Zr), and hexavalent (S, Se, Mo, W) ions (*1–10*). The conductivity of Zr-doped materials is the highest reported so far in this family, with values around 0.025 ohm^{-1} cm^{-1} at 300°C (*4*). Conductivities increase on doping, by virtue of an increase in the number of Na^+ ion vacancies associated with solid solution mechanisms such as:

$$2Na \rightleftharpoons Ca$$

$$3Na \rightleftharpoons Al$$

$$4Na \rightleftharpoons Zr$$

$$Na + P \rightleftharpoons S.$$

There is some evidence that the conductivities may pass through a maximum at compositions around $Na_{2.5}M_yPO_4$, although in most of the systems studied to date, the solid solutions do not extend as far as this composition. The crystal structure of γ-Na_3PO_4 may be regarded as a stuffed antifluorite (*11, 12*); to see this, its formula may be rewritten as

$$Na\,[Na_2PO_4].$$

The part in square brackets is antifluorite like if the PO_4 groups are treated as spherical anions. The Na outside the brackets refers to the "excess" Na^+ ions, which occupy octahedral interstitial sites.

In this paper, the influence of other tetravalent ions, Hf, Ti, Sn, Ce, and Th, as well as Zr, on the formation and conductivity of Na_3PO_4 solid solutions is described; Si-containing materials have also been investigated, but their properties are rather different from those of the other tetravalent systems and will be treated separately.

0022-4596/88 $3.00

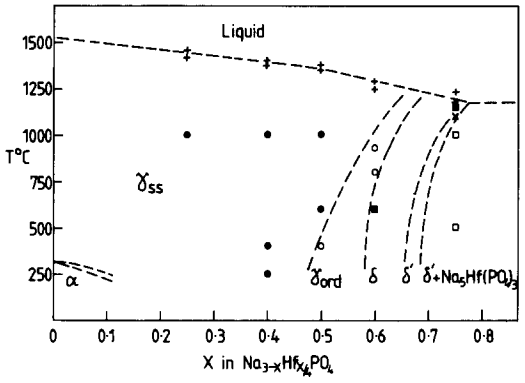

FIG. 1. Phase diagram for the Hf-containing Na_3PO_4 solid solutions. + refers to pellet melting studies; ○, ●, ■, × each refer to different single-phase solid solutions; □ refers to a mixture of phases.

Experimental

Starting materials were Na_2CO_3, $NH_4H_2PO_4$ (Analar), ZrO_2, HfO_2, SnO_2, CeO_2 (all Ventron, 99+%), ThO_2 (Koch-Light, 99.9%), and TiO_2 (tioxide anatase pulp). All were dried at 200–300°C, apart from the $NH_4H_2PO_4$ which was used from the bottle and the anatase pulp which was heated at 1000°C and stored in a vacuum desiccator. Mixtures were prepared in ca. 10-g quantities by weighing out the components, mixing into a paste with acetone in an agate mortar, drying, and firing in Pt crucibles. Firing programs were typically 200°C for 3 hr, 650–800°C for 3 hr, and finally 850–1000°C, depending on composition, for 48 hr. Prior to the final firing, samples were removed from the crucibles and crushed to a fine powder.

Details of the methods used for X-ray powder diffraction, lattice parameter measurements, phase diagram determination, DTA analysis, pellet preparation, electrodes and conductivity cell, and conductivity measurements were as described previously (*9*, *10*). Conductivity data were analyzed as described previously; grain boundary impedances were minimized by attention to firing conditions for the pellets and all the conductivity data reported are bulk conductivity values.

Results

Solid Solutions $Na_{3-x}Hf_{x/4}PO_4$

An extensive range of γ solid solutions and related phases has been prepared, as shown in Fig. 1, which cover the range x = 0 to x = 0.7–0.75. These are stable up to their melting points, 1300–1500°C, depending on x. By comparison, the corresponding Zr γ solid solutions and related phases extend to x = 0.67 at low temperatures, increasing to x = 0.75 at the melting point (*5*). At most temperatures and compositions, the Hf solid solutions have the same cubic structure as the high-temperature, γ, form of Na_3PO_4. The effect of small amounts of Hf on the $\alpha \rightarrow \gamma$ transition in Na_3PO_4 has not been studied but it is shown schematically to fade out with increasing Hf content in Fig. 1, in line with the observed behavior in the Zr-containing solid solutions (*5*).

At large x values, $\gtrsim$0.45, the γ solid solutions undergo various ordering transitions either on cooling or with increasing x. Two ordered polymorphs were identified and labeled, by analogy with corresponding Zr phases, as γ_{ord} and δ. The γ_{ord} phase appears to be cubic, but has a doubled lattice parameter when compared with the high-temperature γ solid solution, as shown by the appearance of extra lines in its X-ray powder pattern. The δ phase is characterized by the splitting of many γ lines and, therefore, is of symmetry lower than cubic. A detailed determination of the composition/temperature ranges of the γ_{ord}/δ phase fields has not been made but these are shown tentatively as separated by dashed lines. The δ phase field is shown subdivided to include a field for the δ' polymorph, which is structurally similar to δ but is characterized by extra line splittings.

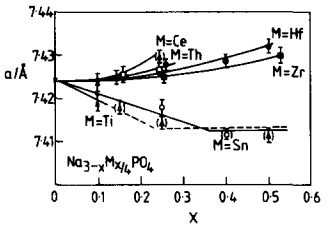

FIG. 2. Lattice parameter, a, against composition, x, for the various M-containing γ solid solutions.

Lattice parameters of the γ solid solutions are given in Fig. 2, together with those of the other γ solid solution series.

Conductivities were measured for three compositions, $x = 0.25$, 0.40 and 0.50 (Fig. 3). The conductivity increases with x and appears to be a maximum at $x = 0.50$; conductivities for $x = 0.60$ (not shown) are between those for $x = 0.50$ and $x = 0.40$. The conductivity data were reversible on thermal cycling, as shown for $x = 0.40$. The conductivity Arrhenius plots show curvature at ~300°C, in common with many other Na_3PO_4-based solid solutions (*9, 10*), and also some evidence of curvature to a region of lower slope below ~100°C. Arrhenius conductivity parameters for each of the γ solid solution series are collected in Table I.

As is the case for the Zr system, the maximum conductivities occur at $x = 0.50$. This composition also coincides approximately with the limit of the γ solid solution field at those temperatures, 50–500°C, at which conductivities are measured; for higher x, the various γ-related phases form. It is not clear whether the decrease in conductivity for $x > 0.50$ is because these compositions transform to γ-related phases or whether an intrinsic maximum in conductivity occurs around $x = 0.5$, irrespective of the particular solid solution polymorph that forms.

Solid Solutions $Na_{3-x}Zr_{x/4}PO_4$

The crystal chemistry of these solid solutions has been well investigated (*5*), but some of the conductivity measurements have been repeated in order to have data over a wider temperature range than given in (*4*). For composition with $x \leq 0.50$, curved Arrhenius plots were obtained, similar to those for the Hf-containing solid solutions (Fig. 3); the data obtained below 300°C are similar to those reported in (*4*).

For compositions with $x > 0.50$, more complex behavior was observed. On a fairly rapid heat/cool cycle (over a few hours) of a sample of $x = 0.53$ with the γ_{ord} structure, the data fall on the upper curve of Fig. 4 and are similar to those obtained with smaller x values. On prolonged annealing at 250–300°C, however, a drop in conductivity of 1–2 orders of magnitude occurred (lower curve in Fig. 4). X-ray data taken at the end of the conductivity measurements showed that the sample had transformed to the ε phase. For this composition, $x = 0.53$, formation of ε was slow. For higher x, it should form more rapidly since it is stable to higher temperatures

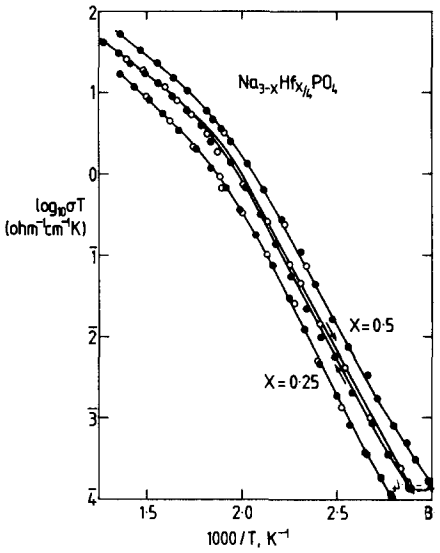

FIG. 3. Conductivity results for Hf-containing Na_3PO_4 solid solutions for three x values; ● and ○ represent data obtained on heating and cooling cycles, respectively.

TABLE I

ARRHENIUS CONDUCTIVITY PARAMETERS

M	x in $Na_{3-x}M_{x/4}PO_4$	Phases present	Region 1 e.g., $120 < T < 250$		Region 2 e.g., $T > 300$	
			E_a/eV	$\log_{10} A$	E_a/eV	$\log_{10} A$
Hf	0.25	γ	0.94	9.1	0.46	4.5
	0.40	γ	0.88	8.8	0.35	3.8
	0.50	γ_{ord}	0.86	8.9	0.38	4.3
	0.60	γ	0.91	9.7	0.32	3.7
Zr	0.25	γ_{ord}	0.94	9.1	0.37	3.7
	0.50	γ_{ord}	0.84	8.6	0.38	4.3
Ti	0.10	γ	1.01	9.3	0.52	4.9
	0.15	$\gamma+$	1.27	12.2	0.50	4.6
	0.25	$\gamma+$	0.86	7.7	0.55	4.9
Sn	0.25	γ	0.91	9.0	0.45	4.5
	0.40	$\gamma+$	0.93	7.0		
Th	0.15	γ	1.00	9.4	0.52	4.8
Ce	0.10	γ	1.02	9.3	0.51	4.6
	0.15	γ	0.90	7.8	0.48	4.5
	0.25	$\gamma+$	0.82	7.2	0.56	5.0

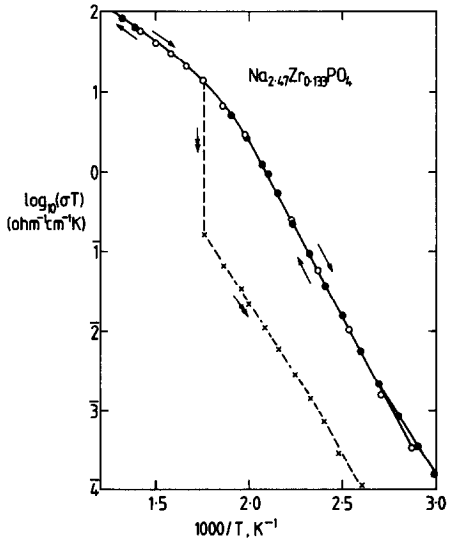

FIG. 4. Conductivity data for a Zr-containing sample, $x = 0.53$, on a rapid heat (●)/cool (○) cycle and after annealing at 300°C followed by slow cooling (×, doubled arrows).

with increasing x (5). It is therefore expected that curves such as the lower one of Fig. 4 would be observed more readily and to higher temperatures with increasing x. Clearly, transformation to the ε phase, with the associated drop in conductivity, is undesirable for any applications that depend on optimization of conductivity.

Solid Solutions $Na_{3-x}Ti_{x/4}PO_4$

The phase diagram for these solid solutions is shown in Fig. 5. A limited range of γ solid solutions forms, extending to ~0.12 at low temperatures, e.g., 400°C, but to ~0.24 at 975°C. As in the Hf system, there was no evidence for the formation of the low temperature polymorph of Na_3PO_4. At the solid solution limit and below ~300°C, the γ solid solutions transform to a low symmetry ε phase. The label ε is given again by analogy with a low symmetry phase observed below 300°C in the Zr system, although, in that case, the ε phase formed only at much higher x, 0.53–0.65. Conductivity data for x

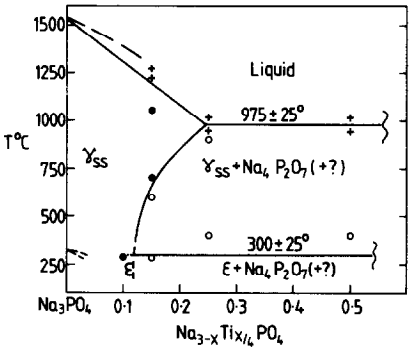

FIG. 5. Phase diagram for the Ti-containing Na_3PO_4 solid solutions. ●, Single phase solid solutions; ○, mixed phases; +, melting behavior of pellets.

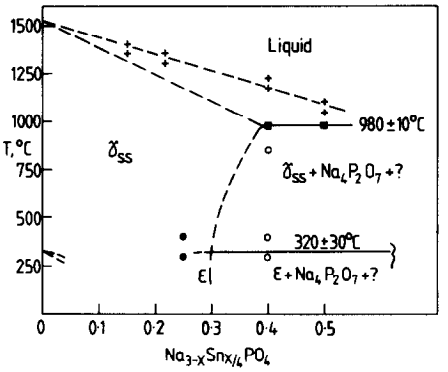

FIG. 7. Phase diagram for the Sn-containing Na_3PO_4 solid solutions. ●, ○, +, As in Fig. 5; ■, melting temperatures determined by DTA.

= 0.1 are given in Fig. 6 and again fall on a curved Arrhenius plot with pronounced sigmoidal character.

Solid Solutions $Na_{3-x}Sn_{x/4}PO_4$

The phase diagram for these solid solutions is shown in Fig. 7. The γ solid solutions are quite extensive, with a limiting x value of 0.35. Again, no evidence of the α polymorph of Na_3PO_4 was seen and at the solid solution limit, the low symmetry ε phase formed below 320°C. Conductivity data for one composition, $x = 0.25$, show a curved Arrhenius plot (Fig. 6) with a small hysteresis between heating and cooling cycles.

Solid Solutions $Na_{3-x}Th_{x/4}PO_4$

The phase diagram for this system (Fig. 8) shows solid solutions extending to x = 0.35. For most of this composition range, the solid solutions have the γ structure, but near to the limit, the ε phase forms at low

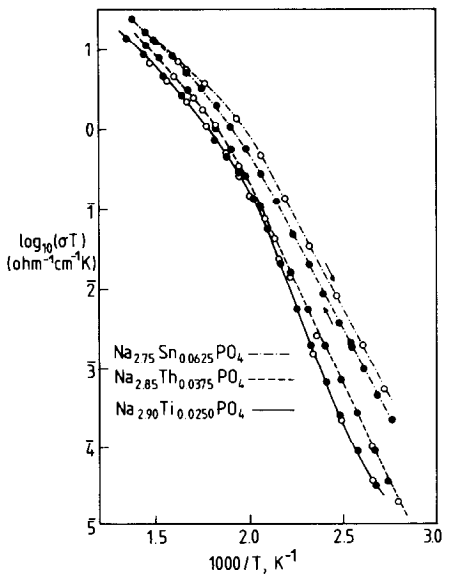

FIG. 6. Conductivity data for Sn-, Th-, and Ti-containing γ-Na_3PO_4 solid solutions.

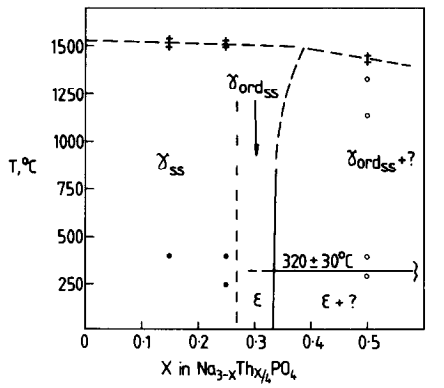

FIG. 8. Phase diagram for the Th-containing Na_3PO_4 solid solutions. Symbols as in Fig. 5.

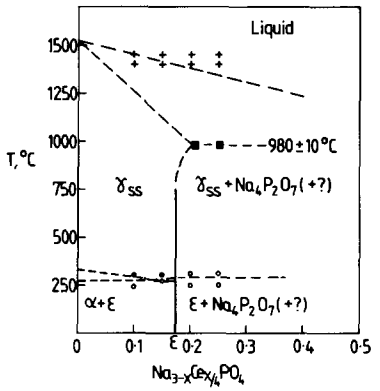

FIG. 9. Phase diagram for the Ce-containing Na_3PO_4 solid solutions. Symbols as in Fig. 7.

temperatures. Above 320°C, this transforms to the γ_{ord} structure, as shown by the presence of extra lines in the X-ray powder pattern, when compared to that of the γ phase. For these limiting x compositions, the γ_{ord} phase appears to be stable essentially up to the melting point, ~1500°C. Conductivity data are shown for one composition, $x = 0.15$, in Fig. 6.

Solid Solutions $Na_{3-x}Ce_{x/4}PO_4$

The phase diagram for this system (Fig. 9) shows a limited range of γ solid solutions, with x values up to ~0.18. At low temperatures, <290°C, the ε phase forms at the solid solution limit and a broad two-phase region of (ε + α) forms at lower x values; this was shown by annealing samples at 250°C for 1 day.

Conductivity data for composition, $x = 0.10$ are shown in Fig. 10. The conductivity behavior observed on a rapid heat/cool cycle is similar to that for the other γ solid solution series, but on annealing at 250°C, a large drop in conductivity is observed and the data follow the lower curve. In this case, X-ray diffraction shows that a mixture of α and ε phases forms during annealing at 250°C. For compositions, $x \geq 0.15$, hysteresis between heating and cooling cycles and a pronounced discontinuity between the high- and low-temperature regions, was observed. This indicates that the order–disorder transition in the γ phase has some first-order character for M = Ce. For these compositions, X-ray diffraction indicated that the samples had the γ structure before and after the conductivity measurements.

An additional complication with this system is that trivalent Ce appears also to be present. Magnetic susceptibility measurements indicate that for composition, $x = 0.1$, a small amount of Ce^{3+}, perhaps 5% of the total Ce content, is present, but this percentage increases markedly with x. For $x = 0.50$, X-ray data indicate the presence of a mixture of phases, including $Na_3Ce(PO_4)_2$; this latter is predominantly a Ce^{3+} phase. It is not clear whether the small amounts of Ce^{3+} indicated for low x values are due to the presence of Ce^{3+} in the solid solution or in another, undetected phase.

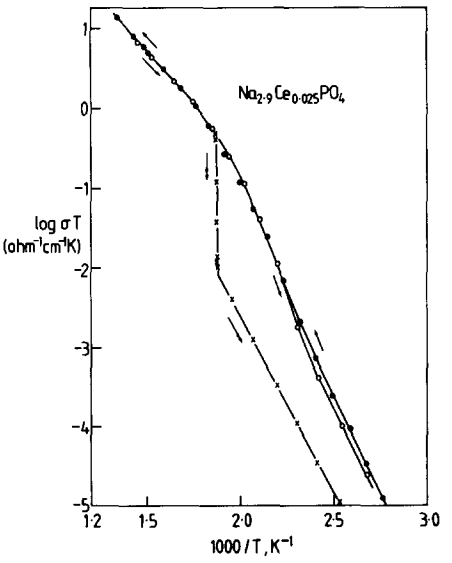

FIG. 10. Conductivity data for a Ce-containing Na_3PO_4 solid solution. Single arrows, first heat/cool cycle; double arrows, second cycle.

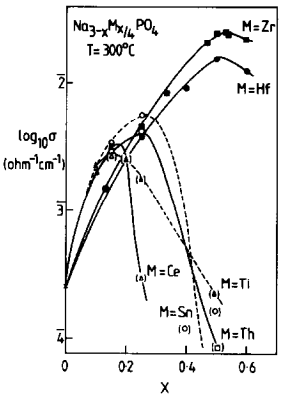

FIG. 11. Conductivity at 300°C for different M-containing solid solutions.

Discussion

The Na_3PO_4 structure is clearly a versatile host structure for tetravalent ions and it is likely that other tetravalent ions that have not been tried, e.g., Ge and U, would also enter the structure. The mechanism of substitution is presumed to be the same as that indicated above for Zr, with the creation of three Na^+ vacancies for each Zr introduced; it would be of interest to do structural studies to confirm this and to locate the tetravalent ions in the γ structure.

The different tetravalent ions substitute to different extents in the sequence Zr > Hf > Sn = Th > Ce > Ti. There appears to be a correlation between the extent of solid solution and the change in lattice parameter with x; from Fig. 2, Zr and Hf show the smallest rate of change in lattice parameter with composition and these are the two tetravalent ions which give the most extensive γ solid solutions.

Conversely, substitution of Ti caused the largest rate of change of a and this was substituted into the γ structure by the smallest amount. Clearly, the size of the introduced ion has a strong bearing on the extent of solid solution; this has been discussed elsewhere (*13*).

In all systems studied, the conductivity increases rapidly with x, as summarized in Fig. 11 for a constant temperature of 300°C. In all cases apart from Zr and Hf, the conductivity is a maximum at the solid solution limit. For Zr and Hf, the maximum in conductivity also coincides approximately with transformation to the noncubic phase and it is not clear whether this effect is responsible for the conductivity maximum or whether the conductivity intrinsically is maximized at $x \cong 0.5$. In the Zr system, almost all the conductivity data for $x < 0.5$ are for the γ_{ord} phase, which is an ordered cubic phase derived from the γ structure. The similarity of these data to those for the Hf system, which are for the γ phase indicates that, as far as conductivity is concerned, there is little difference in properties between γ and γ_{ord} structures.

The formation of the ε phase, on annealing compositions close to the solid solution limit at temperatures of ~300°C, has important implications. In any high-temperature applications, such compositions should be avoided since an irreversible drop in conductivity occurs on prolonged annealing. For the Zr system, the maximum conductivity occurs for $x = 0.53$ and this composition slowly converts to ε on annealing. However, composition $x = 0.50$ appears to be stable at all temperatures and has only slightly less conductivity than $x = 0.53$.

Acknowledgment

We thank the SERC for financial support.

References

1. A.-W. KOLSI, *Rev. Chim. Miner.* **13,** 416 (1976).
2. M. PALAZZI AND F. REMY, *Bull. Soc. Chim. Fr.* **8,** 2795 (1971).
3. J. M. NEWSAM, A. K. CHEETHAM, AND B. C. TOFIELD, *Solid State Ionics* **1,** 395 (1980).

4. S. J. MILNE AND A. R. WEST, *Mater. Res. Bull.* **19,** 705 (1984).
5. S. J. MILNE AND A. R. WEST, *J. Solid State Chem.* **57,** 166 (1985).
6. A. HOOPER, P. MCGEEHIN, K. T. HARRISON, AND B. C. TOFIELD, *J. Solid State Chem.* **24,** 265 (1978).
7. D. M. WIENCH AND M. JANSEN, *Z. Anorg. Allg. Chem.* **486,** 57 (1982).
8. D. MAJIDI, J.-F. BRICE, AND H. KESSLER, *Mater. Res. Bull.* **19,** 1599 (1984).
9. J. T. S. IRVINE AND A. R. WEST, *J. Solid State Chem.* **69,** 127 (1987).
10. J. T. S. IRVINE AND A. R. WEST, *Mater. Res. Bull.* **22,** 1047 (1987).
11. D. M. WIENCH AND M. JANSEN, *Z. Anorg. Allg. Chem.* **461,** 101 (1980).
12. J. M. NEWSAM, A. K. CHEETHAM, AND B. C. TOFIELD, *Solid State Ionics* **1,** 377 (1980).
13. J. T. S. IRVINE AND A. R. WEST, *Solid State Ionics* **27/28** (1988), in press.